

## Encapsulation of natural antioxidants extracted from *Ilex paraguariensis*

Lorena Deladino<sup>a</sup>, Pablo S. Anbinder<sup>a,b</sup>, Alba S. Navarro<sup>a,c,\*</sup>, Miriam N. Martino<sup>a,c</sup>

<sup>a</sup> Centro de Investigación y Desarrollo en Criotecología de Alimentos (CIDCA), CONICET, Fac. Ciencias Exactas, UNLP, 47 y 116, La Plata (1900), Buenos Aires, Argentina

<sup>b</sup> CICPBA, La Plata (1900), Buenos Aires, Argentina

<sup>c</sup> Fac. Ingeniería, UNLP, La Plata (1900), Buenos Aires, Argentina

Received 14 March 2007; received in revised form 15 May 2007; accepted 16 May 2007

Available online 27 May 2007

### Abstract

Yerba mate (*Ilex paraguariensis*) is a beverage traditionally drunk in various countries of South America. It is rich in antioxidant compounds, minerals and vitamins. Aqueous extracts were obtained and characterized by total polyphenols content and antiradical activity. Yerba mate lyophilized extracts were encapsulated with two different systems: calcium alginate and calcium alginate–chitosan. Texture properties of the beads depended on immersion time in  $\text{CaCl}_2$  and in chitosan solutions. Release of the antioxidants in water was measured to analyze the diffusion and kinetic behavior of the system. Sodium citrate was found to be the most effective agent to disintegrate the beads. FT-IR spectra were useful to confirm the interaction of the two polysaccharides. SEM micrographs allowed to select the best drying method for the beads. Encapsulation of yerba mate extracts in alginate and in alginate–chitosan beads is a promising technique for food supplementation with natural antioxidants.

© 2007 Elsevier Ltd. All rights reserved.

**Keywords:** Encapsulation; Antioxidants; Yerba mate; Alginate; Chitosan

### 1. Introduction

Encapsulation is a process in which thin films, generally of polymeric materials are applied to little solid particles, liquid or gases droplets. This method is used to trap active components and release them under controlled conditions. Several materials have been encapsulated in the food industry, among others, aminoacids, vitamins, minerals, antioxidants, colorants, enzymes and sweeteners (Shahidi & Han, 1993).

The encapsulating agents used in this study were chitosan and alginate. Chitosan, obtained from crab exoskeletons, has several polar groups such as  $-\text{OH}$  and  $-\text{NH}_2$  which can act as electron donors. Alginate is extracted from brown seaweed; it has free carboxylic groups which

react with divalent cations, mainly calcium, to form stable gels (King, 1983). Whereas alginates have been largely employed in drug delivery systems, there is increased interest in studying chitosan for its biological applications due to its mucous adhesiveness, no toxicity, biocompatibility and biodegradability (Sinha & Kumria, 2001).

Chitosan and alginate can react together by coacervation due to their opposite charges. The easy solubility of chitosan at low pH is prevented by the alginate network since alginate is insoluble at low pH conditions. The possible dissolution of alginate at higher pH is prevented by the chitosan which is stable at higher pH ranges (George & Abraham, 2006). Alginate–chitosan complexes could solve limitations of individual polyelectrolytes.

In this work, lyophilized extracts of yerba mate (*Ilex paraguariensis*) were encapsulated. This American plant is consumed as an infusion or decoction for its claimed diuretic, anti-inflammatory and mainly for its mild stimulant

\* Corresponding author.

E-mail address: [albanavarro@yahoo.com.ar](mailto:albanavarro@yahoo.com.ar) (A.S. Navarro).

properties (Schinella, Troiani, Davila, de Buschiazzi, & Tournier, 2000). Phytochemical investigations on *Ilex paraguariensis* reported many classes of caffeoyl derivatives and flavonoids as chlorogenic acid, caffeic acid, dicaffeoylquinic acids, rutin, quercetin and kaempferol (Filip, Lotito, Ferraro, & Fraga, 2000). Antiradical efficiency values of these compounds, measured using 2,2-diphenyl-1-picrylhydrazyl (DPPH $\cdot$ ) and *tert*-butyl hydroperoxide (TBH) as radicals, were reported by Sánchez-Moreno, Larrauri, and Saura-Calixto (1998) and Sawa, Nakao, Akaike, Ono, and Maeda (1999), respectively. Both compounds showed high radical scavenging activity.

In foods, antioxidants are added to minimize changes in flavor, aroma, color or nutritional value. Antioxidants can protect the body against damages caused by free radicals and degenerative diseases. Synthetic antioxidants usually employed in industry are effective and stable, but their use is limited in many countries because they are not considered completely safe for human health (Schinella et al., 2000).

Natural antioxidants should be protected from the surrounding medium or the processing conditions during food production. Thus, the objectives of this work were to encapsulate lyophilized yerba mate extracts in calcium alginate beads, with and without a chitosan layer; to analyze the effect of the encapsulating system on the mechanical properties of the beads, to study the matrix influence on the active compound stability and its diffusion properties.

## 2. Materials and methods

### 2.1. Extraction and quantification of polyphenols from yerba mate

#### 2.1.1. Preparation of yerba mate extract

The active component was a lyophilized yerba mate extract obtained in our laboratory (Anbinder, 2004). The extracts were obtained as follows: 1 g of commercial yerba mate (Las Marías, Corrientes, Argentina) was mixed with 100 ml of distilled water in a glass vessel, heated in a thermostatic bath (Haake, Germany) at 100 °C for 40 min. Then the extract was filtered, transferred to dark flasks and cooled in an ice bath. Liquid extracts were frozen at –80 °C for 24 h and lyophilized in a Heto FD4 equipment (Denmark). Lyophilized extracts were put in tightly closed flasks and stored in a desiccator.

#### 2.1.2. Determination of total polyphenols content

Total polyphenols content was determined by Folin-Ciocalteu method (Schlesier, Harwat, Böhm, & Bitsch, 2002). Two milliliters of Na<sub>2</sub>CO<sub>3</sub> (2% w/v) (Anedra, Argentina) were mixed with 200  $\mu$ l of the yerba mate liquid extract and 200  $\mu$ l of Folin-Ciocalteu reagent (Anedra, Argentina, 1:1 diluted). Sample absorbance was measured at 725 nm in a spectrophotometer (Beckman DU 650, USA) after 30 min. Gallic acid (Sigma–Aldrich, USA) was used as a standard and the total phenolic content

was expressed as gallic acid equivalents (mg of gallic acid/g yerba mate). Total polyphenols content was also determined on the lyophilized yerba mate extracts solubilized in water to analyze the effect of lyophilization process.

#### 2.1.3. Antiradical activity quantification

Antiradical activity was determined using DPPH $\cdot$  (Sigma–Aldrich, USA) as a free radical. Different concentrations of yerba mate extract were tested, liquid extract (0.47–15.0 mg yerba mate/ml) and lyophilized samples dissolved in ethanol (0.65–21.0 mg yerba mate/ml). One hundred microliters of each sample were added to 3.9 ml of DPPH $\cdot$ -ethanol solution (25 mg DPPH $\cdot$ /ml ethanol). Absorbance decrease was determined at 517 nm every 0.5 min for 10 min, and then every 15 min until the reaction reached a plateau. For each yerba mate extract concentration tested, the reaction kinetics was plotted (Absorbance vs. time). The final DPPH $\cdot$  concentration for each sample was calculated from a calibration curve. These values and the initial DPPH $\cdot$  amount were used to calculate the percentage of DPPH $\cdot$  remaining at the steady state. These percentages were plotted against yerba mate extract concentration values (Sánchez-Moreno et al., 1998). From this plot, antiradical activity was calculated as the amount of yerba mate extract needed to decrease the initial DPPH $\cdot$  concentration by 50%. This value is commonly expressed as Efficient Concentration (EC<sub>50</sub>), in mg antioxidant per mg DPPH $\cdot$ .

### 2.2. Encapsulation of yerba mate extract

#### 2.2.1. Beads formation

Encapsulating agents used were 2% (w/v) sodium alginate (Protanal, Norway, density: 0.999  $\pm$  0.003 g/ml, viscosity: 1200 cp at 25 rpm) and 1% (w/v) chitosan in acetic acid (Sigma–Aldrich, USA, deacetylation degree higher than 91%, density: 0.996  $\pm$  0.007 g/ml and viscosity: 1900 cp at 25 rpm).

Beads were obtained mixing the active component (1% w/v) with the sodium alginate solution, once homogenized the alginate solution was dropped from a burette to 80 ml of calcium chloride solution (0.05 M). The beads formed were maintained in the gelling bath to harden for different times (0–90 min). Then, they were filtered through a Whatman #1 paper and were washed with buffer solution (acetic-acetate, pH 5.5). Different stabilization times (0–40 min) in air were tested to determine total diffusion time of calcium through the beads. To analyze the effect of an additional layer, beads were immersed in the chitosan solution for 0, 15, 30 or 60 min. The capsules were dried by three different methods; (a) at ambient conditions (20 °C, 65% relative humidity), (b) in oven (80 °C for 24 h) and (c) by freeze drying.

The best conditions for capsule formation were selected according to mechanical properties. The rest of the assays were performed with the selected conditions. They were: 15 min in calcium chloride solution and 15 min in air for

control samples followed by 30 min in chitosan solution for chitosan coated samples.

### 2.2.2. Beads characterization

Humidity content was measured gravimetrically, drying the beads in an oven at 80 °C until constant weight. Values of  $a_w$  were determined using an AquaLab Serie 3 TE (USA) apparatus.

Digital photographs of at least 50 beads were analyzed using the software Global Lab (USA). Average values of radius, roundness and perimeter were measured; *radius* defined as the average values from the center of the area to the perimeter, *roundness* as a value between 0 and 1 indicating how closely the shape of the particle resembles a circle and *perimeter* as the length around the outside edge of the particle.

The beads were observed in a stereomicroscopy Zeiss 47 50 52 – 9001 (Germany) and in a microscopy Zeiss Axiovert 100 A (Germany), both equipped with a photographic camera (Leica).

SEM analysis was performed using a Jeol JSM-6360 (Japan) microscope. Beads were attached to stubs using a two-sided adhesive tape, then coated with a layer of gold (40–50 nm) and examined using an acceleration voltage of 10 kV. SEM–EDAX analysis was done using a scanning electron microscope, Leo 440 (Germany) equipped with an Econ 4 detector (EDAX, USA).

A texture analyzer (TA-TX2i, Stable Micro Systems, UK) was used to determine the mechanical properties of the beads. Compression tests were performed on a Petri dish (9 cm diameter) filled with beads (multiple bead assay), using a plate probe (7.5 cm in diameter) with a speed of 0.5 mm/s. To study the effect of immersion in calcium chloride and stabilization time in air, capsule strength at 50% deformation was measured. Force at 30% deformation was measured to analyze the effect of immersion time in chitosan solution. Assays were performed at least in triplicate. Besides, for chitosan coated beads the compression test for a single capsule was also performed (single bead assay). Means of at least five measurements for each immersion time in chitosan were reported.

Analysis by Fourier transform infrared (FT-IR) spectroscopy was performed on the single components, sodium alginate and chitosan films, and on control and chitosan coated beads. A FT-IR spectrophotometer (Perkin Elmer, Spectrum One, USA) with an attenuated total reflectance (ATR) accessory was used. Samples were scanned from 600 to 4000  $\text{cm}^{-1}$  at a resolution of 4  $\text{cm}^{-1}$ . Each sample was scanned 16 times to obtain the FTIR spectra.

### 2.2.3. Bead destabilization and active agent release

Different matrix destabilizing agents (pH, temperature and chelating agents) were tested. Ten beads of control and chitosan coated samples were placed in test tubes containing 10 ml of the destabilizing agent: HCl 0.1 N, NaOH 0.1 N and sodium citrate 1 and 10% w/v as a calcium chelator were assayed at ambient temperature, and distilled

water was tested at 50 and 100 °C. To facilitate the observation of the structure disintegration of beads, a colorant (methyl violet) was used as the active component. Observations were performed for 24 h.

The release of the active agent in water was quantified by total polyphenols using Folin-Ciocalteu method described in Section 2.1.2. The assay was carried out sinking 20 beads in test tubes with 5 ml of distilled water under continuous agitation. Control and coated chitosan humid beads were tested by triplicate. Measurements were performed at different times between 10 min and 48 h. Percentage release and effective diffusion coefficients ( $D$ ) were calculated.

The amount of lyophilized extract loaded in beads was estimated by dissolving a known amount of capsules in sodium citrate (10% w/v) during 20 min for control capsules and 90 min for chitosan coated beads in an Orbit-Environ Shaker (Lab-Line Instruments, USA) at 37 °C and 125 rpm. The concentrations of lyophilized extract loaded in the beads were determined by Folin-Ciocalteu method. A blank of sodium citrate solution was also performed. The percentage of loading efficiency was calculated with the following equation:

$$\text{Loading efficiency (\%)} = \frac{L}{L_0} \times 100 \quad (1)$$

where  $L$  is the amount of extract determined on the solution of sodium citrate and  $L_0$  is the initial amount of extract dissolved in the alginate solution.

### 2.3. Statistical analysis

Systat-software (SYSTAT, Inc., Evanston, Ill., USA, 1990) version 5.0 was used for all statistical analysis. Analysis of variance (ANOVA) and regression analysis were applied with a significance level of 0.05.

## 3. Results

### 3.1. Quantification of polyphenols and antioxidant activity of yerba mate

Total polyphenol content of the extract was  $62.11 \pm 1.16$  mg of gallic acid/g yerba mate. No significant differences in polyphenol content were found between liquid and lyophilized extracts ( $p < 0.05$ ).

The concentration of antioxidant needed to decrease by 50% the initial substrate concentration ( $EC_{50}$ ) is a parameter widely used to measure the antioxidant power (Sánchez-Moreno et al., 1998). The lower the  $EC_{50}$ , the higher the antioxidant power.  $EC_{50}$  values (in mg of yerba mate per mg of DPPH $\cdot$ ) were:  $0.72 \pm 0.09$  for liquid extract and  $1.05 \pm 0.25$  for lyophilized yerba mate extract. Antioxidant power of liquid and lyophilized yerba extracts were not statistically different ( $p > 0.05$ ). Freeze drying was considered an appropriate technique to store dried extracts, since both polyphenols content and antiradical activity were main-

tained after lyophilization. The yerba mate extracts showed high antiradical power compared with standard gallic acid and other antioxidant components (Brand-Williams, Cuvelier, & Berset, 1995 and Sánchez-Moreno et al., 1998).

Due to the complex analytical technique to measure antioxidant activity by DPPH $\cdot$ , a relationship between both techniques, DPPH $\cdot$  and Folin-Ciocalteu, was analyzed. The following equation was used to fit the experimental data:

$$\text{DPPH}_r = \frac{7.414}{\text{FC}} - 11.332 \quad (2)$$

where DPPH $_r$  is the percentage of remaining DPPH $\cdot$  and FC is the total polyphenols concentration determined by Folin-Ciocalteu method.

Polyphenols content and antiradical activity satisfactory correlated ( $R^2 = 0.978$ ) for different samples of yerba mate extracts (Fig. 1). Thus, for the following active compound quantifications only Folin-Ciocalteu assay was performed due to practical reasons. Relationship between polyphenols and antioxidant activity mainly depends on substrate characteristics; accordingly this analysis should be made for each antioxidant source. This concept agrees with Atoui, Mansouri, Boskou, and Kefalas (2005), who stated that only in some cases this type of correlations could be applied.

### 3.2. Encapsulation of yerba mate extract

#### 3.2.1. Beads formation

Conditions for beads formation were determined from texture measurements. Compression strength was measured at different dipping times in CaCl $_2$ , maximum force of calcium alginate beads sharply increased in the first 15 min and then remained constant ( $p > 0.05$ ), being 38 N the asymptotic value reached. King (1983) suggested that, when calcium and alginate solutions get in contact, a gel is formed immediately at the interface, thus matrix homogeneity depends on the calcium diffusion through the gel network. Diffusion of calcium chloride towards the bead

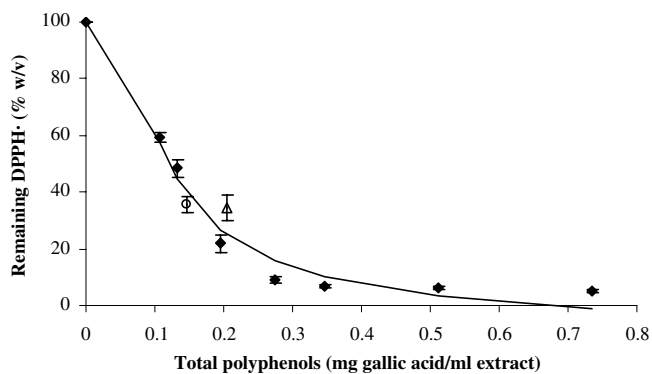


Fig. 1. Correlation between Folin-Ciocalteu and DPPH $\cdot$  methods (◆) for lyophilized yerba mate extract dissolved in water at different concentrations (0.32–3.0 mg extract/ml solution). Yerba mate extract released after 24 h in water from control (△) and chitosan coated (○) beads.

core needed an extra-time to reach a homogeneous distribution, at 5, 15 and 30 min, strength values were 33.6, 52.1 and 58.0 N, respectively. Thus, 15 min in air were enough to get the maximum force ( $p < 0.05$ ).

Immersion times in chitosan solution showed an increase of the strength up to 30 min followed by a decrease in this value (Fig. 2). This behavior was observed in both circumstances when carrying out a multiple bead assay and a single bead assay. The maximum could be associated to a reinforcement of the bead structure; the chitosan could bind to free alginate sites by cooperative ionic bounds until 30 min in chitosan solution. Longer times could cause the shift of the bounded calcium ions by chitosan, leading to a weaker chitosan–alginate gel. Chitosan–alginate complexes capsules were reported to be weak and needed calcium addition to improve structure stability (Bartkowiak & Hunkeler, 1999, 2000; George & Abraham, 2006).

Summarizing, the selected conditions for bead formation were: 15 min in CaCl $_2$  solution and 15 min in air for control alginate beads; for chitosan coated samples, the obtained beads were dipped in chitosan solution for 30 min.

#### 3.2.2. Bead characterization

Longer dipping times in chitosan caused a significant ( $p < 0.05$ ) decrease in bead size (Table 1), however, roundness was not affected ( $p > 0.05$ ). This fact could be attributed to the progressive water loss of the calcium alginate beads due to the chitosan bounding to the matrix. Water loss with chitosan dipping time, determined by  $a_w$  and

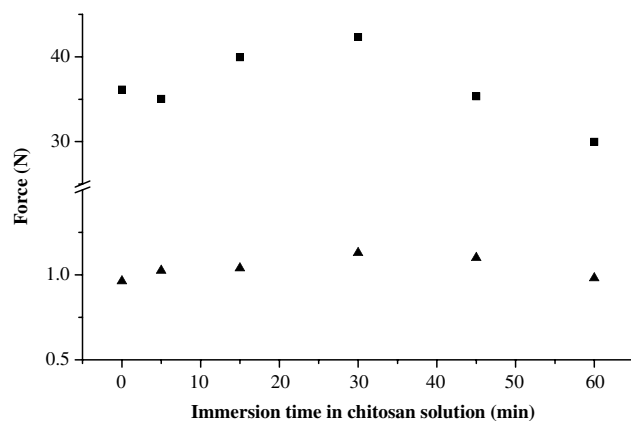


Fig. 2. Chitosan effect on the mechanical properties of capsules: multiple bead assay (■),  $SD_{\max} = 2.48$  and single bead assay (▲),  $SD_{\max} = 0.088$ .

Table 1  
Effect of immersion time in chitosan solution on shape characteristics of capsules.

	Radius (cm)	Roundness	Perimeter (cm)
Control	0.2085 ± 0.005	0.96 ± 0.03	1.300 ± 0.032
15 min	0.2098 ± 0.007	0.97 ± 0.06	1.304 ± 0.095
30 min	0.1916 ± 0.039	0.97 ± 0.03	1.185 ± 0.026
60 min	0.1796 ± 0.005	0.92 ± 0.05	1.142 ± 0.043



Table 2  
Effect of immersion time in chitosan solution on  $a_w$  and water content of capsules

Capsule type	$a_w$		Water content (%)
	Humid beads	Dry beads	Humid beads
Control	0.997 ± 0.002	0.360 ± 0.012	97.38 ± 0.03
15 min in chitosan	0.993 ± 0.001	0.330 ± 0.009	97.28 ± 0.03
60 min in chitosan	0.990 ± 0.002	0.266 ± 0.006	97.09 ± 0.02

water content assays (Table 2), reinforced the above statement.

Microscopic observations of humid beads showed that control ones were spherical with a continuous edge, whereas chitosan coated beads had irregular shape. As seen in Fig. 3, chitosan coated beads show a transparent external layer, attributed to the formation of a chitosan–alginate complex.

Control beads after being dried in an oven (Fig. 4a) had a disc shape and a collapsed center, like a red blood cell. Several authors reported that the collapsed center of dried beads is due to the heterogeneous gelation mechanism evidenced by a dense surface layer and a loose core (Shu & Zhu, 2002; Skjåk-Bræk, Grasdalen, & Smidsrød, 1989). In the case of chitosan coated capsules (Fig. 4c), once dried they became flat with star shape. Two zones could be distinguished, a core attributed to the calcium alginate gel and a surrounding layer due to the alginate–chitosan complex. In both cases (with and without chitosan), lyophilization was not a good drying technique since a pore structure was observed (Fig. 4b and d), leading to a greater exposure of the active compound. Some chitosan beads had pores similar to control, probably due to the lost of the outer layer, and other beads showed a compact membrane (Fig. 4d). Even this layer was not porous, some holes could be observed. Drying under ambient conditions was the selected drying method, because it maintained the spherical shape of the humid beads.

SEM–EDAX analysis allowed the observation of several crystals in the surface of a control capsule (Fig. 5a and b). These crystals could be attributed to sodium chloride, taking into account the similar distributions of chlorine dots (Fig. 5c) and sodium dots (Fig. 5d) in the corresponding mineral mapping. As seen in Fig. 5e, calcium mapping shows a different pattern compared to chlorine and sodium mapping. During gel formation, calcium ions interact with alginate to form the matrix, thus sodium ions are free to interact with chloride ions from the gelling bath. After drying of capsules, sodium chloride crystals could have remained over the surface. However, the composition of these crystals needs to be confirmed by other techniques like X-rays.

Hydrocolloids, sodium alginate and chitosan have similar structure so their FTIR spectra have characteristic bands attributed to their saccharide units (Fig. 6a and b). Between 3450 and 3490  $\text{cm}^{-1}$  spectra show a band attributed to the –OH groups, the glucose ring appears around 1060 and 1150  $\text{cm}^{-1}$  (Jansson-Charrier, Saucedo, Guibal, & Le Cloirec, 1995). Chitosan has typical bands due to the amino and amide groups present in its structure, at 1650 (amida I) and 1543  $\text{cm}^{-1}$  (amida II), respectively. Control (c) and chitosan coated (d) beads, and alginate film showed similar spectra, this match was attributed to the high proportion of alginate in the capsules (Fig. 6). The band around 1050  $\text{cm}^{-1}$  present in chitosan film arose in chitosan coated beads (d), this band is attributed to skeletal

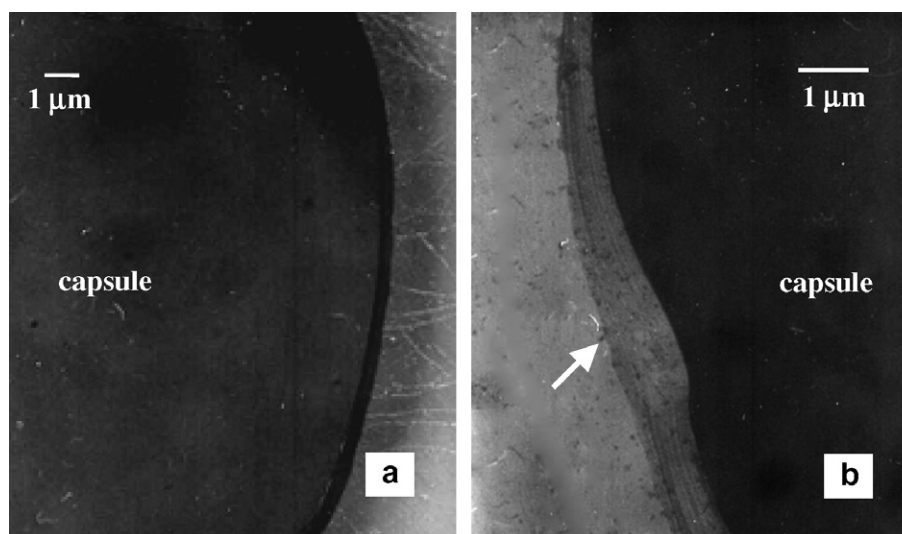


Fig. 3. Microphotographs of cross sections: (a) control capsule, (b) chitosan coated capsule. The white arrow shows the chitosan membrane.

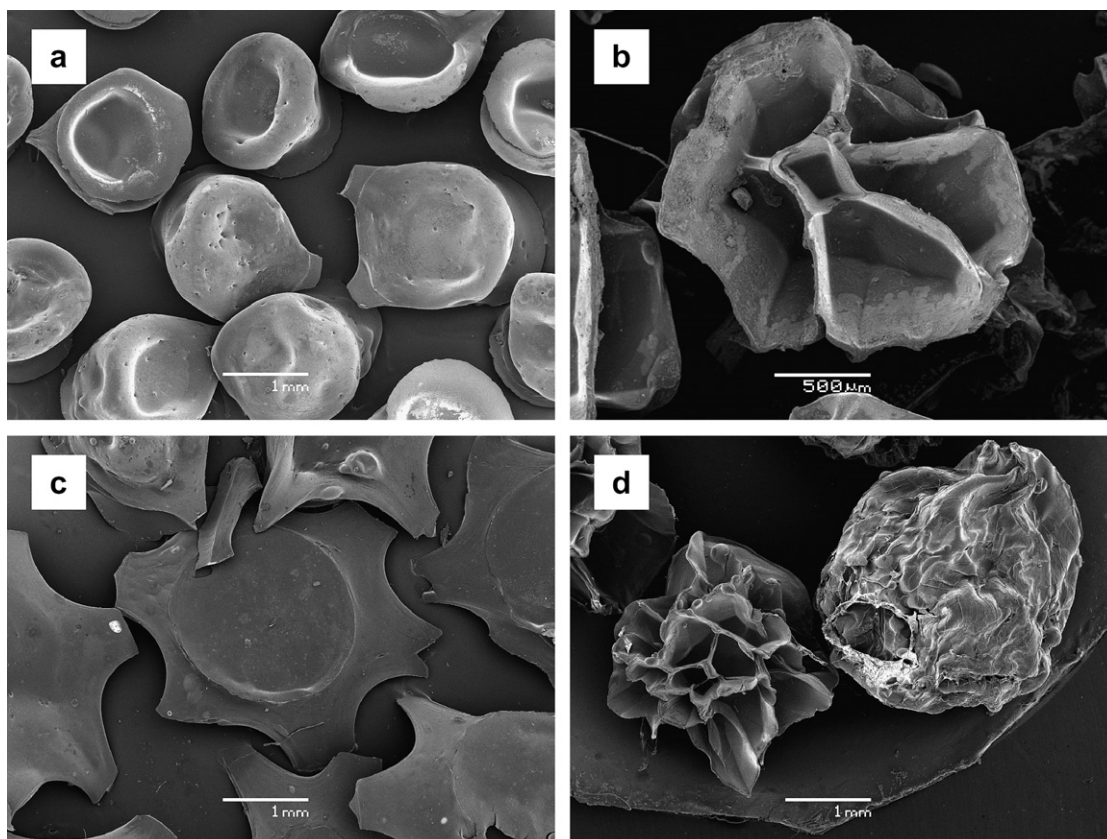


Fig. 4. SEM microphotographs of control (a) dried in oven and (b) lyophilized beads; and alginate–chitosan (c) dried in oven and (d) lyophilized beads.

vibrations involving the CO stretching. Besides, new bands around  $1117$  and  $1240\text{ cm}^{-1}$  were distinguished, indicating an electrostatic interaction between the protonated amino groups of chitosan and the dissociated carboxylate groups of sodium alginate, respectively (Sarmiento, Ferreira, Veiga, & Ribeiro, 2006; Smitha, Sridhar, & Khan, 2005). Wavenumber shifts of typical bands appearing in pure hydrocolloids (a and b) were also found in bead spectra: the band appearing at  $1590\text{ cm}^{-1}$  in pure alginate was found at  $1620\text{ cm}^{-1}$  in both type of beads. However, according to Smitha et al. (2005), this band, in the chitosan coated beads, could be also attributed to a symmetric  $\text{—NH}_2\text{C}$  deformation.

### 3.2.3. Bead destabilization and active agent release

Destabilization of the encapsulation system is required for total release of the active compounds. Several conditions were analyzed: temperature, hydrochloric acid, sodium hydroxide and sodium citrate media. Results are shown in Table 3. Sodium citrate destabilized the calcium alginate gel;  $\text{Ca}^{+2}$  ions of the network were exchanged by  $\text{Na}^+$  ions, weakening the gel structure. This destabilizing agent showed a lower effect on chitosan beads compared to control ones (Table 3); after 20 min of immersion in the solution, control beads were dissolved and capsules with chitosan remained intact. Ninety minutes were needed to disintegrate the chitosan coated beads, even more, after this time some remaining “ghosts” could be visualized.

Similarly, Gåserød, Sannes, and Skjåk-Bræk (1999) stated that chitosan–alginate membrane governs capsule structure when a sequestrant agent as sodium citrate is used.

Loading efficiencies of the two types of capsules were significantly different ( $p < 0.05$ ) (Table 4). Control capsules showed a high load of active compound ( $>85\%$ ); similarly, Pasparakis and Bouropoulos (2006) obtained values higher than  $80\%$  in verapamil loaded microcapsules. As in chitosan coated beads the entrapment was lower than expected, the process was analyzed to determine in which stage the active compound was lost. Total polyphenols content was measured in sodium chloride and in chitosan solutions after the beads were removed from each solution. Active compound losses were mainly produced during immersion in chitosan. Similar results were obtained by Bajpai and Tankhiwale (2006), who attributed this behavior to the porous structure of the beads derived from the low molecular weight of the two polymers.

Percentage release was calculated based on the actual entrapped yerba mate extract (Table 4). The lower release of chitosan coated beads was attributed to higher retention characteristics due to the alginate–chitosan membrane (Pasparakis & Bouropoulos, 2006) and the possible interaction between chitosan and polyphenols from the extract (Popa, Aelenei, Popa, & Andrei, 2000).

Antioxidant activity and polyphenols content were determined after 24 h of release in water to evaluate whether encapsulation technique could modify antioxidant

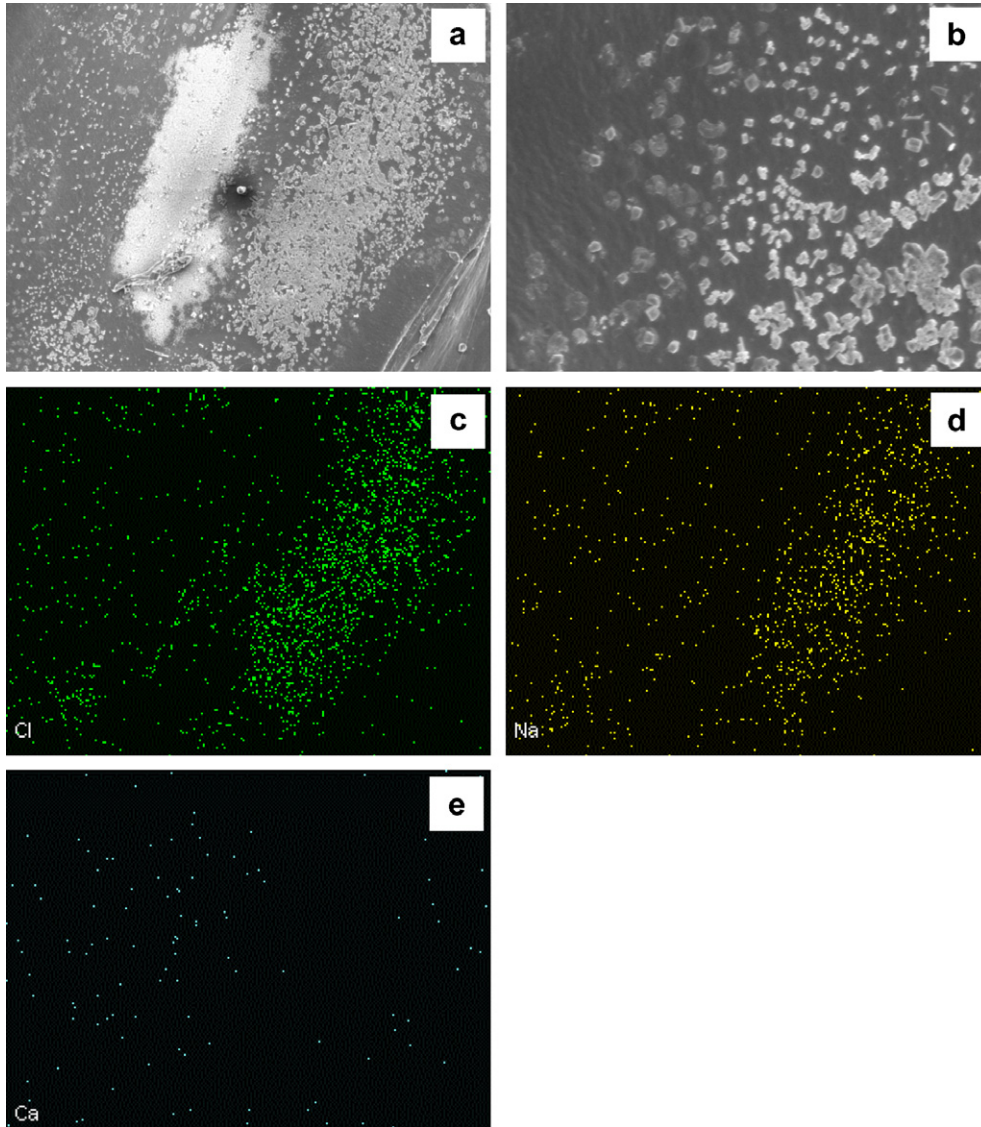


Fig. 5. SEM–EDAX microphotographs of the same section of a control bead dried in oven at 100 $\times$ : (a) SEM image; (b) SEM image at 442  $\times$ ; (c) chloride mapping; (d) sodium mapping; (e) calcium mapping.

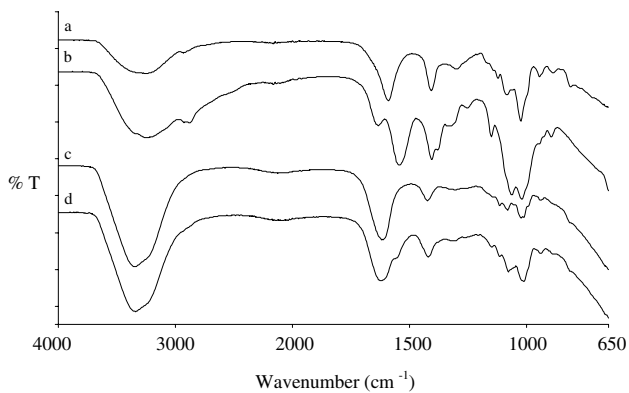


Fig. 6. FT-IR spectra: (a) alginate film, (b) chitosan film, (c) control bead and (d) chitosan coated bead.

power of the loaded extract. Results for control and chitosan coated beads satisfactorily fitted the correlation

between polyphenols and antioxidant activity (Eq. 2) calculated from yerba mate extract (Fig. 1). Thus, encapsulation technique maintained antioxidant power of the active compound.

Fig. 7 shows  $M_t/M_\infty$  as a function of time, where  $M_t$  is the mass of polyphenols released at time  $t$  and  $M_\infty$  is the maximum mass of polyphenols released after capsule disintegration with sodium citrate. Two zones were distinguished, a first increasing zone and a last stage independent of time. Popa et al. (2000), working on the release of polyphenols from chitosan–polyphenols complexes, also found two domains on the release kinetics. To determine the time at which a change of release mechanism was produced, the release rate at each time was calculated:

$$r = \frac{\Delta M}{\Delta t} = \frac{M_{j+1} - M_j}{M_\infty(t_{j+1} - t_j)} \quad (3)$$



Table 3  
Effect of different destabilization agents on beads integrity

Treatment	Control beads	Chitosan coated beads
Temperature (50 and 100 °C)	There is no effect on the structure. Higher temperature, more antioxidant release	There is no effect on the structure. The release is lower than in control
pH acidic	There is no effect on the structure	There is no effect on the structure
pH alkaline	Integrity loss after 24 h	White shell with liquid interior
Sodium citrate	Integrity loss after 20 min	There is no effect on the structure up to 90 min

Table 4  
Efficiency of different encapsulation systems

Capsule type	Parameters	
	Loading efficiency (%)	Release in water (%)
Control	87.1 ± 0.2	47.4 ± 0.3
Chitosan coated	48.5 ± 0.5	35.5 ± 0.1

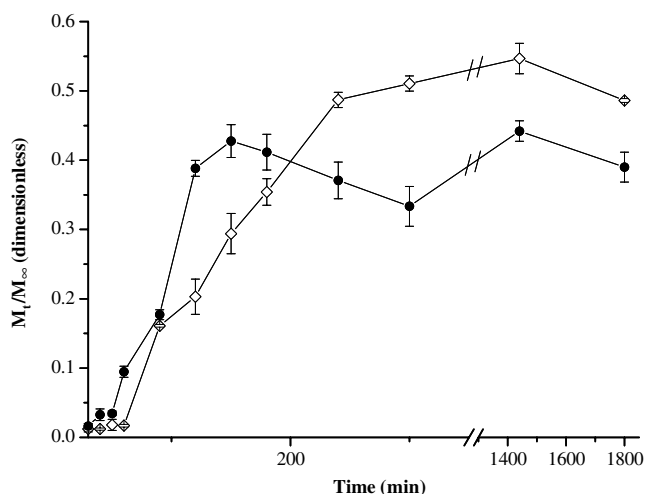


Fig. 7. Release curve:  $M_t/M_\infty$  vs. time; chitosan coated beads (●) and control beads (◇).

where  $r$  is the rate at average time  $t = (t_j + t_{j+1})/2$ ,  $\Delta M$  is the polyphenols released over a  $\Delta t$  time interval. The second zone characterized by a constant release rate was reached at 210 min for chitosan coated beads and at 300 min for control ones; this stage corresponded to a zero order mechanism.

To evaluate the release mechanism, a semi-empirical equation was applied to the first part of the kinetic curve:

$$\frac{M_t}{M_\infty} = kt^n \quad (4)$$

where  $k$  is a constant related to structural and geometric characteristics of the beads, and  $n$  is the exponent indicative of the release mechanism. These parameters were calculated using the relative release values corresponding to the time dependent part of the curve for each system. Eq. 4 fitted experimental data giving correlation coefficients higher than 0.91 (Table 5). Both capsule systems gave  $n$  values higher than 1, associated to different mechanisms acting together. According to several authors (Llabot,

Table 5  
Kinetic parameters obtained from release curves:  $D$  is the effective diffusion coefficient,  $n$  and  $k$  are constants

Capsule type	Kinetic parameters		
	$n$	$k \times 10^5$ (s <sup>-n</sup> )	$D \times 10^4$ (cm <sup>2</sup> /s)
Control <sup>a</sup>	2.21	0.40	1.65
Chitosan coated <sup>b</sup>	2.09	1.34	2.50

<sup>a</sup> Values determined between 30 and 240 min.

<sup>b</sup> Values determined between 30 and 150 min.

Manzo, & Allemandi, 2004; Pothakamury & Barbosa-Cánovas, 1995; Sumathy & Ray, 2002), the parameter  $n$  can take a range of values indicating the type of transport of the active agent. When  $n = 0.5$ , the active agent is released by simple Fickian diffusion. When  $n = 1.0$ , diffusion is described as *case II* transport; in this case, the rate of solvent uptake by the polymer is largely determined by the rate of swelling and relaxation of the polymer chains. *Super case II* transport occurs when  $n > 1.0$  and is related to the plasticization of the polymer system, a reduction of the attractive forces between chains that increases the mobility, thus the active compound release is facilitated (Llabot et al., 2004). In our case, both systems behaved similarly, an initial chain plasticization that allowed diffusion and then a swelling and relaxation mechanisms acting together. The fact that chitosan beads released a lower relative amount of antioxidant could be attributed to the interaction between polyphenols compounds and chitosan (Popa et al., 2000). Chitosan coated beads did not delay transport rate, as it was expected. Experimental observations showed that several chitosan coated beads, once dipped in water were disrupted. We attributed this behavior to the fracture of the external layer of chitosan owing to the higher relaxation and water uptake of the calcium alginate gel inside the chitosan–alginate layer of the beads.

The effective diffusion coefficient ( $D$ ) was calculated according to the following equation (Pasparakis & Bouropoulos, 2006):

$$D = \left( \frac{k}{4(\pi R^2)^n} \right)^{1/n} \quad (5)$$

where  $R$  is the mean radius of the beads.

Values of diffusion coefficients are shown in Table 5. Similar  $D$  values were found by Pasparakis and Bouropoulos (2006) for wet alginate–chitosan mixed beads containing verapamil and by Bajpai and Tankhiwale (2006), who stud-



ied the release of vitamin B<sub>2</sub> from calcium alginate/chitosan multilayered beads.

#### 4. Conclusions

Yerba mate has high antiradical power and high total polyphenols content becoming in a natural source of antioxidants. A good correlation between Folin-Ciocalteu and DPPH<sup>•</sup> techniques facilitated practical quantification of active compound content.

Alginate beads formation and texture properties depended on immersion time in Ca<sup>2+</sup>, their further stabilization in air and immersion time in chitosan when applied.

The presence of a uniform external layer in chitosan coated beads was observed by different microscopic techniques. Moreover, the formation of chitosan–alginate complex was evidenced by FTIR.

SEM allowed to select the appropriate drying method to preserve the active compound. Lyophilization was not a good drying technique since a porous structure for the control was obtained. This fact increased external surface favoring active compound exposure.

High load of active compound (>85%) was obtained in control beads. However, the entrapment in chitosan coated beads was lower (around 50%) since active compound was lost during immersion in chitosan. The percentage released was higher for control beads since polyphenols could be retained in chitosan–alginate membrane. However, maximum release in water was achieved at shorter times for chitosan coated beads compared with control ones. Diffusion behavior did not follow a Fickian model, a Super case II transport was observed in both encapsulating systems.

The analyzed encapsulation method allowed to tailor the release of natural antioxidants of yerba mate, depending on the presence of a chitosan coating layer. Controlling amount and rate of active agents release makes encapsulation suitable for different applications in the food industry.

#### References

- Anbinder, P. S. (2004). Encapsulation of yerba mate antioxidants. Food Technology Degree Thesis, (pp. 22–28), Universidad Nacional de Mar del Plata, Balcarce, Argentina.
- Atoui, A. K., Mansouri, A., Boskou, G., & Kefalas, P. (2005). Tea and herbal infusions: Their antioxidant activity and phenolic profile. *Food Chemistry*, *89*, 27–36.
- Bajpai, S. K., & Tankhiwale, R. (2006). Investigation of dynamic of vitamin B<sub>2</sub> from calcium alginate/chitosan multilayered beads: Part II. *Reactive and Functional Polymers*, *66*(12), 1565–1574.
- Bartkowiak, A., & Hunkeler, D. (1999). Alginate-oligochitosan microcapsules: A mechanistic study relating membrane and capsule properties to reaction conditions. *Chemical Materials*, *11*, 2486–2492.
- Bartkowiak, A., & Hunkeler, D. (2000). Alginate-oligochitosan microcapsules. II. Control of mechanical resistance and permeability of the membrane. *Chemical Materials*, *12*, 206–212.
- Brand-Williams, W., Cuvelier, M. E., & Berset, C. (1995). Use of a free radical method to evaluate antioxidant activity. *Lebensmittel-Wissenschaft-und-Technologie*, *28*, 25–30.
- Filip, R., Lotito, S. B., Ferraro, G., & Fraga, C. G. (2000). Antioxidant activity of *Ilex paraguariensis* and related species. *Nutrition Research*, *20*(10), 1437–1446.
- Gåserød, O., Sannes, A., & Skjåk-Bræk, W. (1999). Microcapsules of alginate–chitosan. II. A study of capsule stability and permeability. *Biomaterials*, *20*, 773–783.
- George, M., & Abraham, E. (2006). Polyionic hydrocolloids for the intestinal delivery of protein drugs: Alginate and chitosan – a review. *Journal of Controlled Release*, *114*, 1–14.
- Jansson-Charrier, M., Saucedo, I., Guibal, E., & Le Cloirec, P. (1995). Approach of uranium sorption on chitosan and glutamate glucan by IR and C NMR analysis. *Reactive & Functional Polymers*, *27*, 209–221.
- King, A. H. (1983). Brown Seaweed Extracts (Alginates). In M. Glicksman (Ed.). *Food Hydrocolloids* (Vol. 3, pp. 115). Boca Raton, FL: CRC Press, Chapter 3.
- Llabot, J. M., Manzo, R. H., & Allemandi, D. A. (2004). Drug release from carbomer: Carbomer sodium salt matrices with potential use as mucoadhesive drug delivery system. *International Journal of Pharmaceutics*, *276*, 59–66.
- Pasparakis, G., & Bouropoulos, N. (2006). Swelling studies and in vitro release of verapamil from calcium alginate and calcium alginate–chitosan beads. *International Journal of Pharmaceutics*, *323*, 34–42.
- Popa, M. I., Aelenei, N., Popa, V. I., & Andrei, D. (2000). Study of the interaction between polyphenolic compounds and chitosan. *Reactive and Functional Polymers*, *45*, 35–43.
- Pothakamury, U. R., & Barbosa-Cánovas, G. V. (1995). Fundamental aspects of controlled release in foods. *Trends in Food Science and Technology*, *6*, 397–406.
- Sánchez-Moreno, C., Larrauri, J. A., & Saura-Calixto, F. (1998). A procedure to measure the antiradical efficiency of polyphenols. *Journal of the Science of Food and Agriculture*, *76*, 270–276.
- Sarmiento, B., Ferreira, D., Veiga, F., & Ribeiro, A. (2006). Characterization of insulin-loaded alginate nanoparticles produced by ionotropic pre-gelation through DSC and FTIR studies. *Carbohydrate Polymers*, *66*, 1–7.
- Sawa, T., Nakao, M., Akaike, T., Ono, K., & Maeda, H. (1999). Alkylperoxy radical-scavenging activity of various flavonoids and other phenolic compounds: Implications for the anti-tumor-promoter effect of vegetables. *Journal of Agriculture and Food Chemistry*, *47*, 397–402.
- Schinella, G. R., Troiani, G., Davila, V., de Buschiazzo, P. M., & Tournier, H. A. (2000). Antioxidant effects of an aqueous extract of *Ilex paraguariensis*. *Biochemical and Biophysical Research Communications*, *269*, 357–360.
- Schlesier, K., Harwat, M., Böhm, V., & Bitsch, R. (2002). Assessment of antioxidant activity by using different in vitro methods. *Free Radical Research*, *36*(2), 177–187.
- Shahidi, F., & Han, X. (1993). Encapsulation of food ingredients. *Critical Reviews in Food Science and Nutrition*, *33*(6), 501–547.
- Shu, X. Z., & Zhu, K. J. (2002). The release behavior of brilliant blue from calcium-alginate gel beads coated by chitosan: The preparation method effect. *European Journal of Pharmaceutics and Biopharmaceutics*, *53*, 193–201.
- Sinha, V. R., & Kumria, R. (2001). Polysaccharides in colon-specific drug delivery. *International Journal of Pharmaceutics*, *224*, 19–38.
- Skjåk-Bræk, G., Grasdalen, H., & Smidsrød, O. (1989). Inhomogeneous polysaccharide ionic gels. *Carbohydrate Polymers*, *10*, 31–54.
- Smitha, B., Sridhar, S., & Khan, A. A. (2005). Chitosan–sodium alginate polyion complexes as fuel cell membranes. *European Polymer Journal*, *41*, 1859–1866.
- Sumathy, S., & Ray, A. R. (2002). Release behaviour of drugs from tamarind seed polysaccharide tablets. *Journal Pharmacy and Pharmaceutical Sciences*, *5*(1), 12–18.